

Supporting Information

Na₃V₂(PO₄)₂F₃@C dispersed within carbon nanotube frameworks as high tap density cathode for high-performance sodium-ion batteries

Chao Shen,^a Hai Long,^a Gencheng Wang,^a Wei Lu,^b Le Shao,^{*c} and Keyu Xie^{*a}

^a *State Key Laboratory of Solidification Processing, Center for Nano Energy Materials, Northwestern Polytechnical University and Shaanxi Joint Laboratory of Graphene (NPU), Xi'an 710072, China.*

Email: kyxie@nwpu.edu.cn

^b *University Research Facility in Materials Characterization and Device Fabrication, The Hong Kong Polytechnic University, Hong Kong, China.*

^c *Shaanxi Coal and Chemical Technology Institute Co., Ltd, Jinye Road, Xi'an 710070, China.*

Email: shaole@sxcti.com

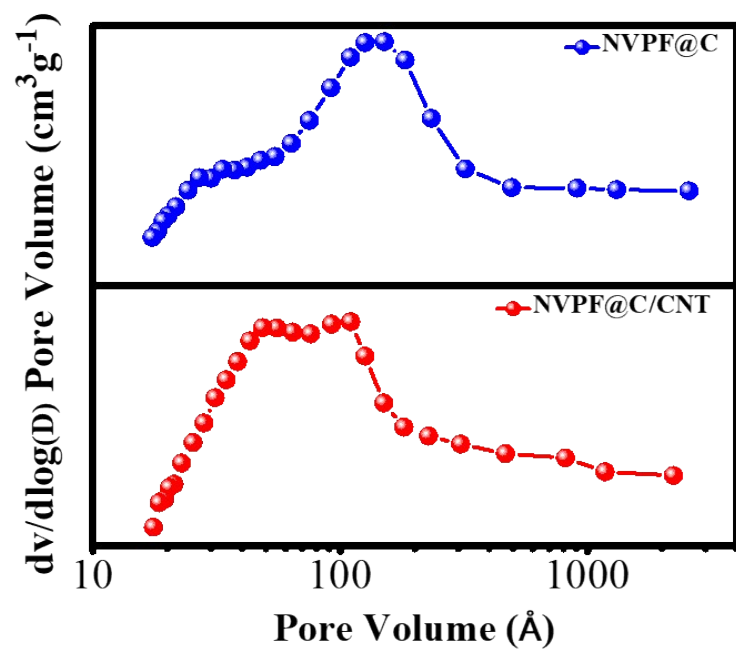


Figure S1. The plot of pore-size distribution of NVPF@C and NVPF@C/CNTs, respectively.

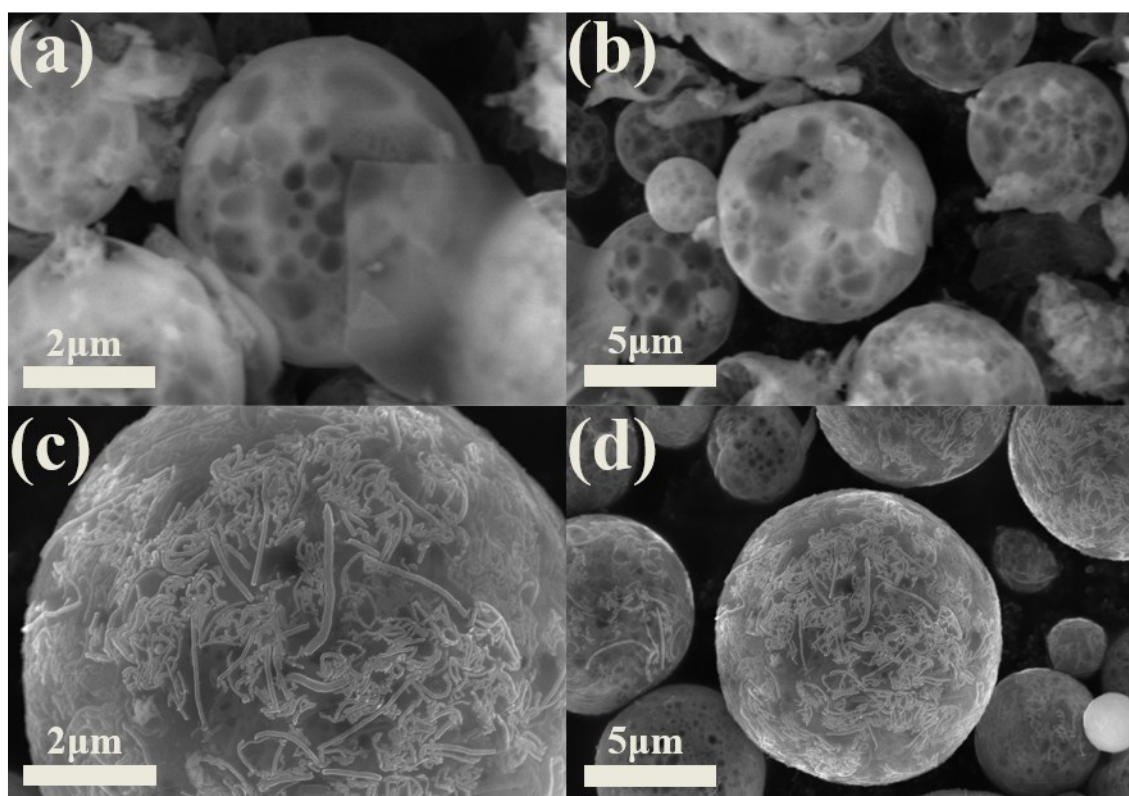


Figure S2. SEM images of the precursor (a, b) NVPF@C and (c, d) of NVPF@C/CNTs.

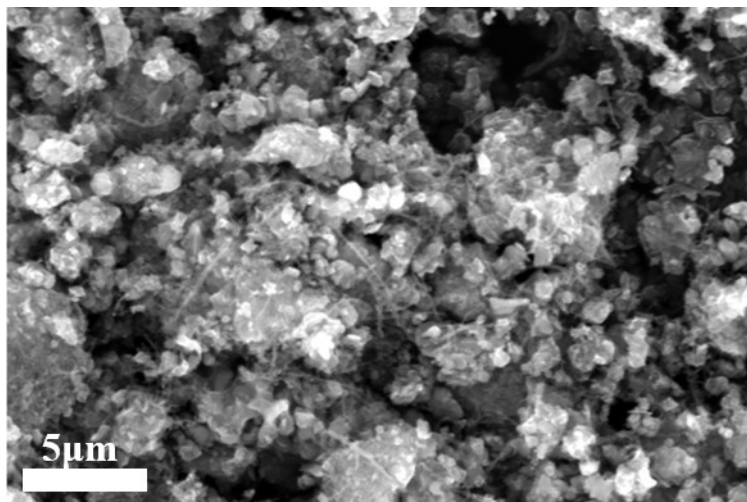


Figure S3. The SEM images of BM-NVPF@C/CNTs samples with an irregular shape of secondary particle and nano-sized of primary particle.

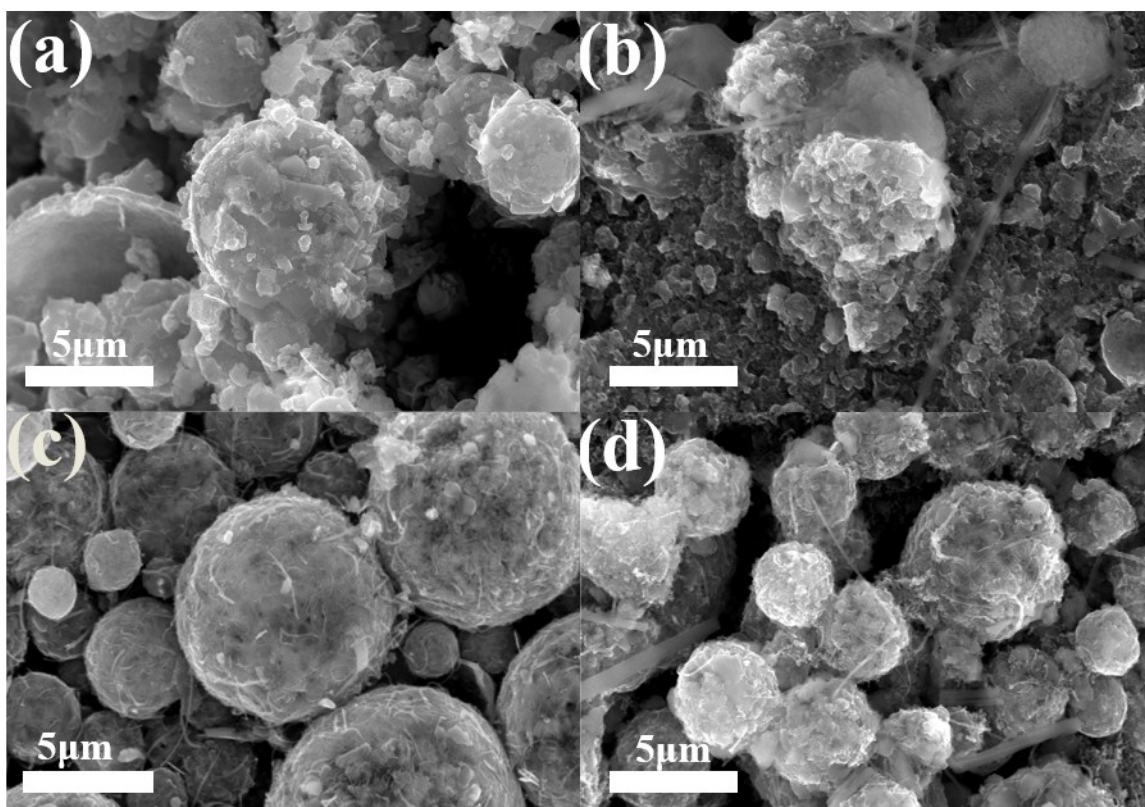


Figure S4. SEM images of (a) NVPF@C and (c) NVPF@C/CNT before cycle; SEM images of (b) NVPF@C and (d) NVPF@C/CNTs, after discharge and charge at 10 C for 300 cycles.

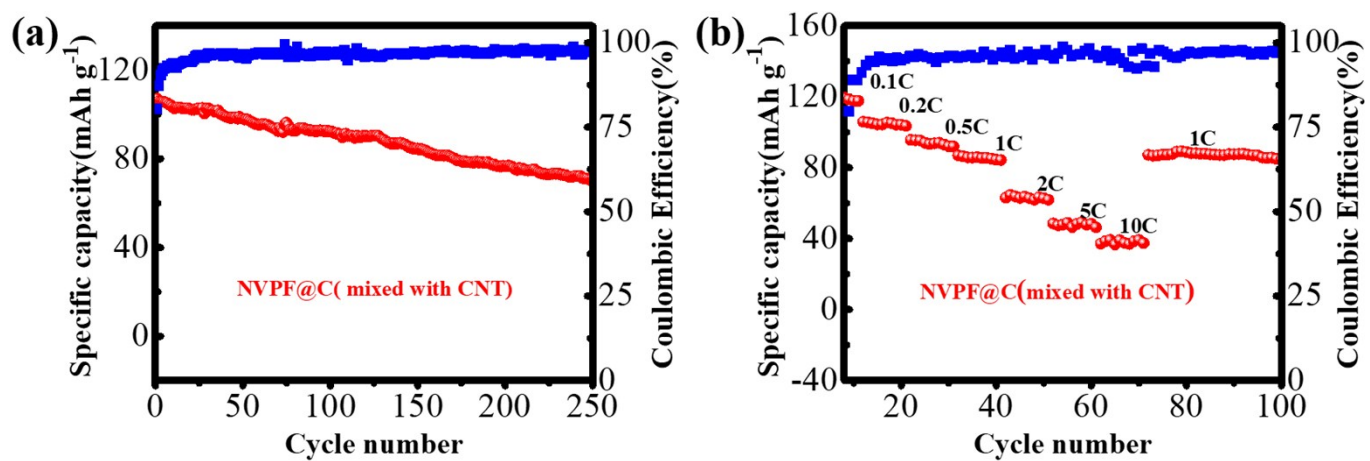


Figure S5. (a) Cycle performance and Coulombic efficiency of the physical mixture of NVPF@C and CNTs for 250 cycles; (b) Rate capability at various current rates for the physical mixture of NVPF@C and CNTs.

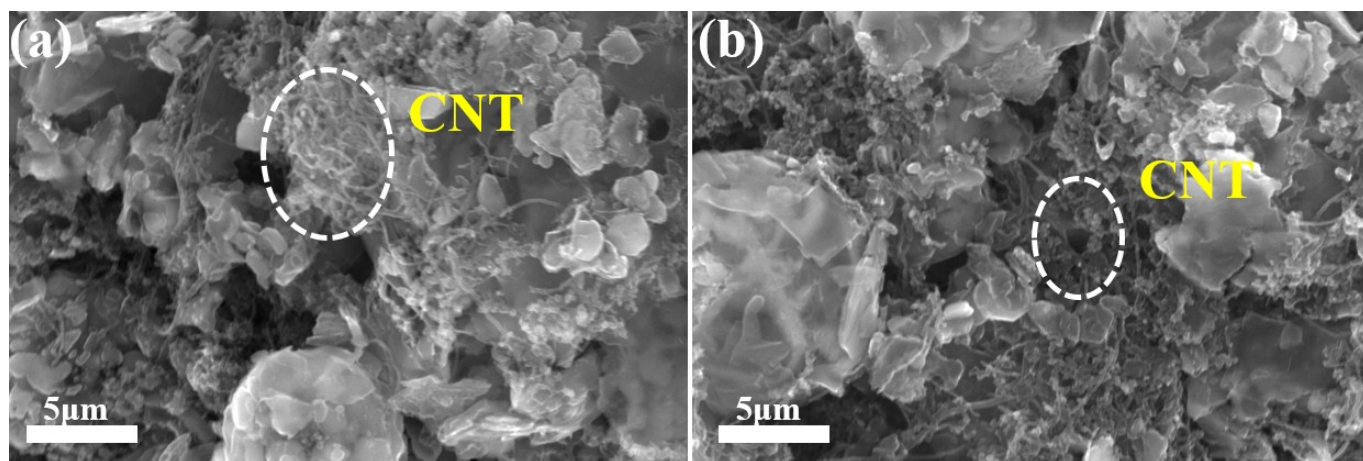


Figure S6. (a-b) SEM images of the physical mixture of NVPF@C and CNTs.

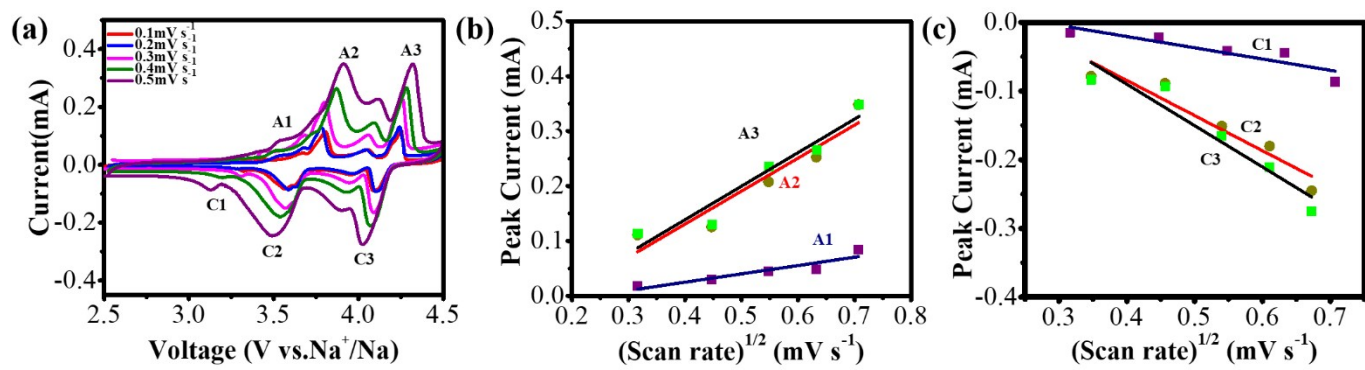


Figure S7. (a) CV curves at different scan rates of the NVPF@C; (b, c) show the relationship between the peak current (I_p) and the square root of the scan rate ($n^{1/2}$).